JOURNAL OF AGRICULTURAL AND FOOD CHEMISTRY

Structure and Stability of the Potato Cysteine Protease Inhibitor Group (Cv. Elkana)

LAURICE POUVREAU, TOOS KROEF, HARRY GRUPPEN, GERRIT VAN KONINGSVELD, LAMBERTUS A. M. VAN DEN BROEK, AND ALHONS G. J. VORAGEN*

Department of Agrotechnology and Food Sciences, Laboratory of Food Chemistry, Wageningen University, 6700 EV Wageningen, The Netherlands

The conformational stability of potato cysteine protease inhibitor (PCPI), the second most abundant protease inhibitor group in potato tuber, was investigated at ambient temperature and upon heating using far- and near-UV circular dichroism spectroscopy, fluorescence spectroscopy, and differential scanning calorimetry (DSC). The PCPI isoforms investigated have a highly similar structure at both the secondary and the tertiary level. PCPI isoforms show structural properties similar to those of the potato serine protease inhibitor group and the Kunitz type soybean trypsin inhibitor, a known β-II protein. Therefore, PCPI isoforms are also classified as members of the β-II protein subclass. Results show that the thermal unfolding of PCPI isoforms does not follow a two-state mechanism and that at least one intermediate is present. The occurrence of this intermediate is most apparent in the thermal unfolding of PCPI 8.3 as indicated by the presence of two peaks in the DSC thermogram. Additionally, the formation of aggregates (>100 kDa), especially at low scan rates, increases the apparent cooperativity of the unfolding.

KEYWORDS: PCPI; thermal unfolding; β-II protein; aggregation

INTRODUCTION

Protease inhibitors are ubiquitously abundant in tubers and plant seeds (*1*). In higher plants, several gene families of protease inhibitors have been characterized, particularly those constituting the serine protease inhibitors from *Leguminosae*, *Solanaceae*, and *Graminae* (*2*).

In potatoes, a wide range of protease inhibitors is expressed (*3*). Potato tuber contains approximately 1.5% (w/w) protein on a fresh weight basis (*3*). In cv. Elkana, a variety used for the industrial processing of potato starch, protease inhibitors represent approximately 50% of the total amount of soluble protein present in the tuber (cv. Elkana) of which the potato cysteine protease inhibitor (PCPI) group represents approximately 12% (*4*).

Cysteine proteases are widely distributed among living organisms; the most abundant is the papain family. This family consists of papain and related plant proteases, such as chymopapain and bromelain. In humans, well-known cysteine proteases are cathepsins B, H, and L. Cysteine proteases are involved in a variety of physiological processes such as protein degradation, antigen presentation, bone resorption, and hormone processing (*5*). They also play a role in many pathological processes including tumor invasion and metastasis (*6*). Therefore, specific cysteine protease inhibitors, such as PCPI, may have considerable potential for diagnosis and treatment. In some cases, insects have adapted their digestive proteases to combat the plant endogenous inhibitors (*7*). Therefore, for crop protection, it may also be of interest to genetically modify plants with cysteine protease inhibitors genes in order to broaden their range of inhibitors.

PCPI isoforms are potent inhibitors of cysteine proteases such as papain but show also activity again trypsin (*4*). PCPIs are monomeric proteins with a molecular mass varying from 20 to 22 kDa. Eight isoforms of PCPI, with isoelectric pH values varying from pH 5.8 to 9.4, have been characterized in potato juice (cv. Elkana) (*4*).

In industrial processes, potato proteins are recovered as a byproduct (*8*). This is done by an acidic heat treatment of the potato protein containing liquid and results in irreversibly precipitated proteins (*8*). Understanding the conformational changes of these potato proteins induced by temperature may help to understand the mechanism of the ensuing aggregation and precipitation. However, data about pH and heat stability of PCPIs are absent. The aim of the present study was, therefore, to investigate the structural properties and the thermal stability of the three most abundant isoforms of PCPI (*4*).

MATERIAL AND METHODS

Preparation of PCPI Solutions. PCPI isoforms 8.3, 8.6, and 9.4 were purified from cv. Elkana as described previously (*4*). An additional chromatofocusing purification step was included, using a Polybuffer Exchanger 118 column (60 cm × 1.6 cm) (Amersham Biosciences, Uppsala, Sweden). The column was equilibrated with 0.025 M

* To whom correspondence should be addressed. Tel: +31 317 483209. Fax: +31 317 484893. E-mail: Fons.Voragen@wur.nl.

10.1021/jf050306v CCC: $30.25
Published on Web 06/11/2005

diethanolamine−HCl buffer, pH 9.4, for PCPI 8.3 and 8.6 and with 0.025 M triethanolamine−HCl, pH 11.0, for PCPI 9.4. The fractions corresponding to PCPI 8.3, 8.6, and 9.4 (*4*) were loaded onto the column. The protein was eluted using Polybuffer 96-HCl (pH 7.0) (dilution factor 1:10) for PCPI 8.3 and 8.6 and using Pharmylate-HCl (pH 8.0) (dilution 1:45) for PCPI 9.4 (Amersham Biosciences). The absorbance of the eluates was monitored at 280 and 320 nm. Appropriate fractions (20 mL) were collected and pooled. The Polybuffer was removed by hydrophobic interaction chromatography using a HP Phenyl Sepharose column (10 cm × 2.6 cm) (Amersham Biosciences). After purification, the purified PCPIs 8.3, 8.6, and 9.4 were dialyzed at 4 °C against a 95 mM sodium acetate buffer, pH 4.0 (ionic strength, 15 mM). After dialysis, the samples were frozen in small volumes and stored until use at a concentration of 1 mg/mL.

Soybean trypsin inhibitor (STI) was purchased from Fluka (art. no. 93618). STI was dissolved in 9 mM sodium phosphate buffer (pH 7.0) and dialyzed against the same buffer overnight at 4 °C.

Protein Purity. Sodium dodecyl sulfate−polyacrylamide gel electrophoresis (SDS−PAGE), with and without β-mercaptoethanol, and IEF electrophoresis were performed with a Pharmacia PhastSystem according to the instructions of the manufacturer using Gradient 8−25% and IEF 3−9 Phastgels, respectively. Gels were stained according to the Coomassie brilliant blue R-250 staining procedure provided by the manufacturer.

Protein Quantification. Because the sequence of PCPI 8.3 is known (*9*), the protein concentration of PCPI 8.3 was determined by measuring its absorbance at 280 nm in the presence of 6 M GndHCl, using a theoretical extinction coefficient of 17210 M^{-1} cm^{-1} based on its sequence. The protein content of PCPI 8.3, 8.6, and 9.4 was also determined using the Bradford assay (*10*). To be able to use bovine serum albumin (BSA) instead of PCPI 8.3 (being a representative PCPI) as a standard a normalization was used to correct the difference in response between BSA and PCPI 8.3.

Mass Spectrometry. Matrix-assisted laser desorption/ionization time-of-flight mass spectrometry (MALDI-TOF-MS) analysis in the linear mode was performed using a Voyager DE RP instrument (Perseptive Biosystems, Framingham, MA) as described previously (*4*).

Gel Filtration. The ÄKTA explorer protein chromatography system and the columns used for the protein purification were from Amersham Biosciences. The absorbance of the eluates was monitored at 280 nm.

A Superdex 75 (30 cm × 0.32 cm) was used to determine if aggregation was taking place during heating and to estimate the size of possible aggregates. The column was equilibrated with 100 mM sodium phosphate buffer (pH 7.5) and operated at a flow rate of 0.5 mL/min. Proteins used for calibration were as follows: ribonuclease A (13.7 kDa), chymotrypsinogen A (25.0 kDa), ovalbumin (43.0 kDa), BSA (67.0 kDa), and Blue dextran (2000 kDa). The protein samples (0.2−0.8 mg/mL) were heated with a scan rate of 30 °C/h up to 85 °C and cooled to 20 °C before applying them onto the column.

Spectroscopic Measurements. All samples were filtered through a 0.22 μm filter before spectroscopic measurements. Between two measurements, the cuvette was thoroughly cleaned with Nanopure water and subsequently rinsed with ethanol.

Far-Ultraviolet Circular Dichroism (Far-UV CD). Far-UV CD spectra of 0.2 mg/mL of PCPI in 95 mM sodium acetate buffer (pH 4.0) were recorded on a Jasco J-715 spectropolarimeter (Jasco Corp., Tokyo, Japan) at temperatures ranging from 20 to 85 °C with intervals of approximately 5°, with a heating rate of 30 °C/h. The temperature was measured in the sample using a thermocouple wire. Starting from 20 °C, the proteins were heated to the desired temperature and equilibrated for 3 min at this temperature before the wavelength scans were recorded. Quartz cells with an optical path length of 0.1 cm were used. The scan range was 260−190 nm, the scan speed was 50 nm/min, the data interval was 0.2 nm, the bandwidth was 1.0 nm, the sensitivity was 20 mdeg, and the response time was 0.125 s. Spectra were recorded 10-fold and averaged. Spectra were corrected using a spectrum of a protein-free sample obtained under identical conditions. Noise reduction was applied using the Jasco software. The spectra were analyzed from 240 to 190 nm to estimate the secondary structure content of the protein, using a nonlinear regression procedure (*11*). Spectra were fitted using the reference spectra of poly-lysine in the α-helix, β-strand, and random coil conformation (*12*) and the spectrum of β-turn structures, extracted from 24 proteins with known X-ray structures (*13*). Changes in secondary structure of PCPI during heating were also monitored by measuring the ellipticity at 222 nm as a function of temperature. The ellipticity at 222 nm is usually correlated with the α-helical content (*14*).

Near-UV CD. Near-UV CD spectra of 0.6 mg/mL PCPI in 95 mM sodium acetate buffer (pH 4.0) were recorded on a Jasco J-715 spectropolarimeter (Jasco Corp.) at 20 °C. Spectra were recorded 30-fold and averaged. Spectra were corrected using a spectrum of a protein-free sample obtained under identical conditions. A quartz cell with an optical path length of 1.0 cm was used. The scan interval was 250−350 nm, the scan speed was 100 nm/min, the data interval was 0.2 nm, the bandwidth was 1.0 nm, the sensitivity was 20 mdeg, and the response time was 0.125 s.

Fluorescence Spectroscopy. Fluorescence spectra of 0.2 mg/mL solutions of PCPI in 95 mM sodium acetate buffer (pH 4.0) at 20 °C were recorded on a Perkin-Elmer Luminescence Spectrophotometer LS 50 B (Perkin-Elmer Corp., Boston, MA). Excitation was done at 285 nm, and the resulting emission was measured from 290 to 405 nm with a scan speed of 100 nm/min. Both the excitation and the emission slits were set at 3.5 nm. Spectra were recorded 3-fold and averaged. Spectra were corrected using a spectrum of a protein-free sample obtained under identical conditions.

Changes in the tertiary structure of PCPI during heating were also monitored by measuring the changes in fluorescence intensity at 300 nm as a function of temperature using a Varian Cary fluorimeter (Varian Cary Inc., Palo Alto, CA). A maximum emission at 305 nm when excited at 285 nm is represensative of tyrosine emission, which is not dominated by tryptophan emission (*15*). Therefore, following the changes in fluorescence at 300 nm indicates changes in the local environment of the protein (*16*).

Fourier Transformed Infrared (FTIR) Spectroscopy. Attenuated total reflection infrared (ATR-IR) spectra were recorded on a Bio Rad FTS 6000 spectrometer equipped with a DTGS detector (BioRad Laboratories Inc., Cambridge, MA). Typically, 50 μL of a 0.8 mg/mL PCPI samples in 9 mM phosphate buffer (pH 7.0) was transferred onto a germanium crystal (1 cm × 8 cm) and dried under air to remove excess water. Next, the crystal was placed in such a way in the light beam that six total reflections were obtained. Spectra were accumulated at ambient temperature in the spectral region of 4000 to 800 cm^{-1} with a spectral resolution of 0.5 cm^{-1} prior to zero-filling and Fourier transformation, using a speed of 5 kHz and a filter of 1.2 kHz. Typically, 100 spectra were accumulated and subsequently averaged. A spectrum representing atmospheric water was subtracted from the sample spectra. All samples were prepared and analyzed at least in duplicate. Spectra were deconvoluted in order to analyze the underlying absorption bands using $K = 2.4$ and a full width at half-height of 24 cm^{-1} using the deconvolution function available in the BioRad software (BioRad Laboratories Inc.).

Differential Scanning Calorimetry (DSC). DSC measurements were performed on a VP-DSC Microcalorimeter (MicroCal Inc., Northampton, MA). Solutions containing 0.6 mg/mL PCPI in 95 mM sodium acetate buffer (pH 4.0) were heated from 20 to 85 °C with a scan rate of 30 °C/h.

To investigate the reversibility of the unfolding, the samples were heated with a scan rate of 30 °C/h to a temperature just after the transition was complete. The sample was subsequently cooled to 20 °C and reheated to 85 °C with the same scan rate.

RESULTS

Protein Architecture. The purity and the molecular mass of the three main isoforms of PCPI were studied using SDS−PAGE and MALDI-TOF-MS. SDS−PAGE under reducing conditions showed a single band at approximately 20 kDa for each isoform (data not shown).

To determine the molecular mass of these three PCPI isoforms more precisely, MALDI-TOF-MS experiments were carried out (**Figure 1**). The MALDI-TOF-MS spectra showed two peaks

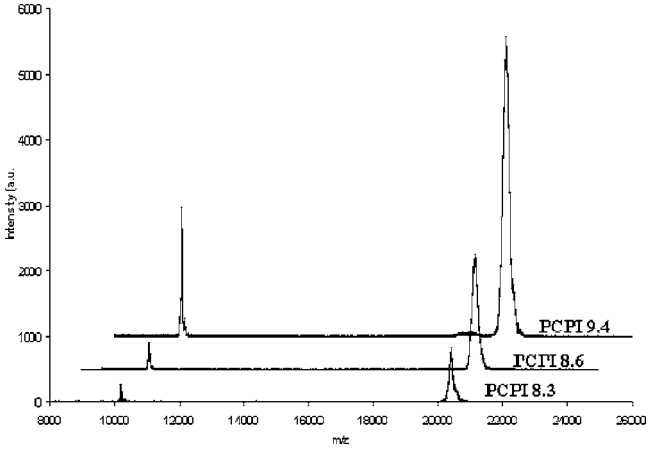

Figure 1. MALDI-TOF-MS spectra of PCPI isoforms.

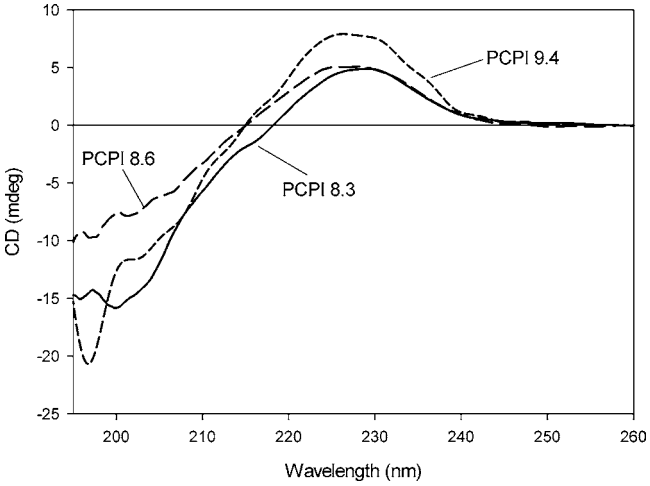

Figure 2. Far UV CD spectra of PCPI 8.3 (solid), PCPI 8.6 (long dashes), and PCPI 9.4 (short dashes) (pH 4.0) at 20 °C. Spectra were recorded 10-fold and averaged.

at 10216 and 20433 Da for PCPI 8.3, at 10064 and 20128 Da for PCPI 8.6, and at 10066 and 20132 Da for PCPI 9.4, respectively. The two peaks correspond to the doubly and singly charged ions of the same protein. The similarity in molecular mass between the isoforms is in accordance with previous results (*4*).

Structural Properties at Ambient Temperature. To study the structural properties of the three isoforms of PCPI at pH 4.0, far-UV CD, near-UV CD, fluorescence, and ATR-IR spectra of all PCPI isoforms were recorded. **Figure 2** shows far-UV CD spectra of the three isoforms of PCPI at pH 4.0. The spectra for PCPI 8.6 and 9.4 have similar characteristics with a zero crossing at 214.5 nm, a minimum around 197 nm, and a maximum at 228 nm. The spectrum of PCPI 8.3 is slightly deviated from the two others by the fact that it shows a zero crossing at a somewhat higher wavelength (≈217 nm). The large similarities between the spectra indicate that the isoforms have a highly similar structure. Fitting of the spectra using reference spectra for the α-helix, *β*-sheet, *β*-turn, and random coil was not successful; therefore, no secondary structure can be assigned for PCPI isoforms. It has to be noticed that far-UV CD spectra of PCPI isoforms shows high similarities to those of potato serine protease inhibitor (PSPI) isoforms (*17*). Near-UV CD spectra give an indication of the interactions of aromatic side chains with other side chain groups and peptide bonds, reflecting the tertiary structure of a protein (*18*). **Figure 3** shows the near-UV CD spectra of the three isoforms of PCPI at pH 4.0 (20

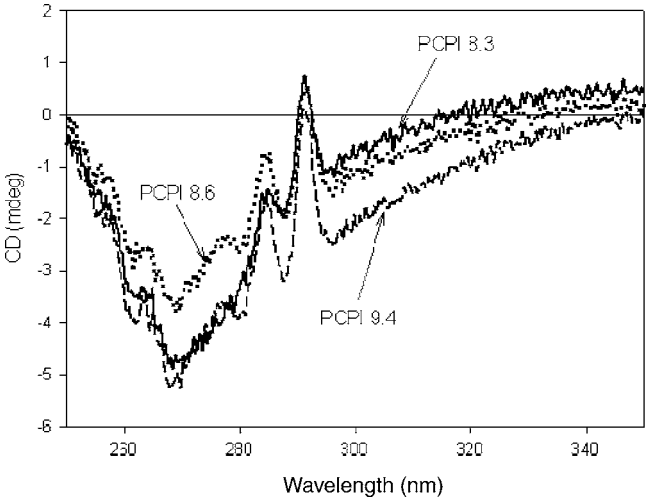

Figure 3. Near UV CD spectra of PCPI 8.3 (solid), PCPI 8.6 (dot), and PCPI 9.4 (dashes) (pH 4.0) at 20 °C. Spectra were recorded 30-fold and averaged.

°C). All spectra show extremes at 292, 285, and 268 nm, although the peak at 285 nm for PCPI 8.3 is very weak as compared to those for PCPI 8.6 and 9.4. The remarkable sharpness of the peaks at 285 and 292 nm indicates a compact and rigid protein structure (*14*). The peak at 292 nm points to the presence of tryptophan residues, whereas the peaks at 285 and 268 nm indicate the presence of tyrosyl and phenylalanine residues, respectively. In comparison to the near-UV CD spectra of PSPI (*17*), the peaks of PCPI isoforms are sharper and more distinct. In the case of PCPI 8.3, the presence of these three peaks is in accordance with its amino acid sequence (ref *9*; SwissProt, O24383), which shows the presence of one tryptophan, seven tyrosyl, and nine phenylalanyl residues. PCPI 9.4 has been previously described (*19*), but no amino acid sequence was given. PCPI 8.6 has been described as a new cysteine protease inhibitor (*4*), and also of this protein, no amino acid sequence is available. From the near-UV CD spectra, it is, however, clear that both PCPI 8.6 and PCPI 9.4 contain at least one tryptophan and one tyrosyl residues. By comparing peak intensities at 285 and 292 nm between PCPI isoforms, we assume that PCPI 8.6 and 9.4 contain at least a similar amount (or higher) of tyrosyls residues.

Fluorescence spectroscopy can give information about the solvent accessibility of the chromophores (tryptophan, tyrosine, and phenylalanine). Therefore, the fluorescence spectrum is sensitive to local changes in the tertiary structure of a protein (*20*). Because the near-UV CD spectra of PCPI isoforms all showed the presence of tryptophan residues according to the near-UV CD spectra, tryptophan fluorescence emission spectra were recorded. Surprisingly, no tryptophan emission maxima were observed for all three isoforms (**Figure 4**). It has to be noticed that, for most native proteins containing tryptophan and tyrosyl residues, their fluorescence emission excited at 280−285 nm is dominated by the tryptophan emission where the band maxima vary in wavelength between 328 and 350 nm (*15*). The tyrosine emission was hard to detect even though the ratio Tyr:Trp is high, like in human serum albumin where the ration is 17:1 (*21*). The quenching in tryptophan emission may be explained by the presence of strong hydrogen bonds between the side chains of the tryptophan with that of phenylalanine (*16*). Therefore, tyrosine emission spectra were recorded. These spectra (**Figure 4**) showed, for all three isoforms, a maximum at 305 nm, indicating that some of the tyrosyl residues are located on the periphery of the protein and that they are not

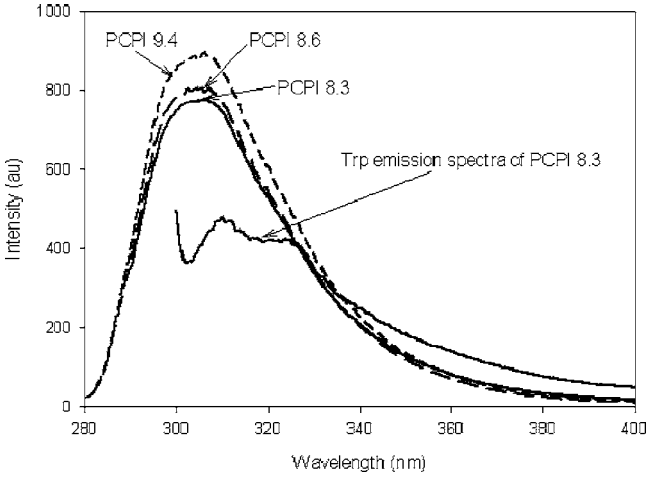

Figure 4. Tyrosine fluorescence emission spectra of PCPI 8.3 (solid), PCPI 8.6 (long dashes), and PCPI 9.4 (short dashes) (pH 4.0) at 20 °C. Spectra were recorded 3-fold and averaged.

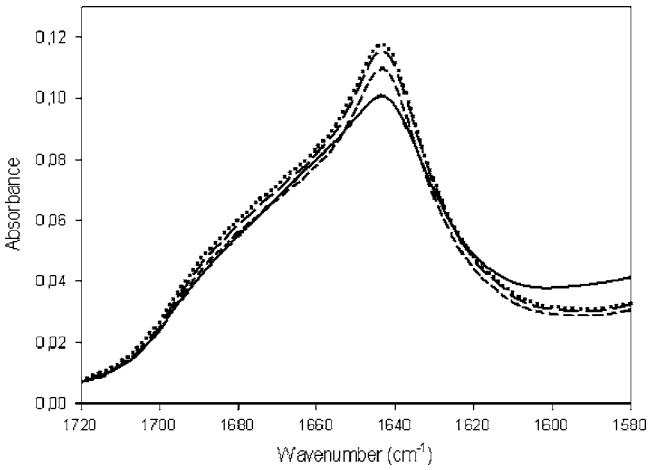

Figure 5. Amide I region of the ATR-IR spectra of PCPI 8.3 (long dashes), PCPI 8.6 (short dashes), PCPI 9.4 (dot), and STI (solid) (pH 4.0). One hundred spectra were accumulated and averaged subsequently.

near the tryptophan residue, since no photon transfer is occurring from the tyrosyl to the tryptophan residue (*16*). PCPI isoforms show a very rare fluorescence behavior where the tyrosine emission is dominating the tryptophan one, similar to a 33 kDa protein from spinach photosystem II (*16*). Even though PSPI isoforms show similar far- and near-UV CD spectra, as well as a similar amount of tyrosyl residues (*17*), PSPI isoforms do not show any tyrosine emission when excited at 285 nm but only trytophan emission.

IR spectroscopy is another method to investigate protein secondary structure based on molecular vibration of specific bonds, such as the C═O vibrations in the amide I band (1600−1700 cm^{-1}). FTIR spectroscopy, therefore, can give information on the secondary structure (*22*). **Figure 5** shows the amide I band of the infrared spectra of both PCPI isoforms and the Kunitz type STI, of which the X-ray structure has revealed that it contains approximately 2% α-helix, 38% β-sheet, 23% β-turn, and 37% unordered structure (*23*, *24*). The spectra indicate that there is a very high degree of similarity between STI and PCPI isoforms. Deconvolution of the spectra revealed the presence of a major band at 1642 cm^{-1}, which indicates the presence of both unordered structure and short β-sheets (*25*). Other deconvoluted bands at 1689 and 1624 cm^{-1} and at 1672 and 1662 cm^{-1} can be observed, indicating the presence of β-sheets and

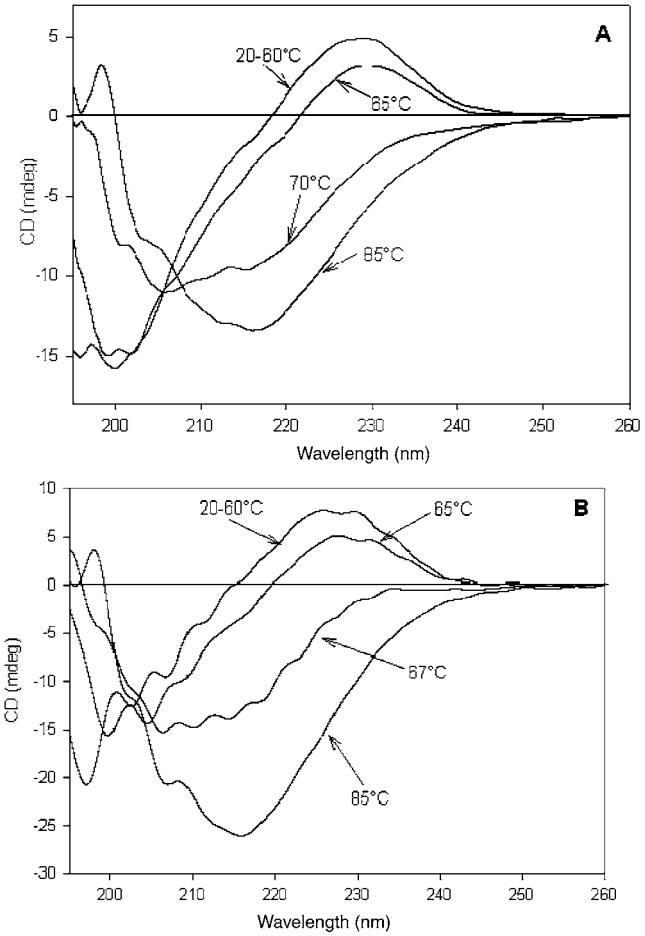

Figure 6. Far UV CD spectra of PCPI 8.3 (**A**) and PCPI 9.4 (**B**) (pH 4.0) at various temperatures. After 3 min at the desired temperatures, spectra were recorded 10-fold and averaged.

turns, respectively (*25*). The intensity of these bands shows that STI is somewhat richer in β-sheet and β-turns than PCPI isoforms. In comparison to PSPI (*17*), PCPI isoforms seem even more similar to STI (*26*) than the PSPI group members.

Thermal Stability. The thermal stability of PCPI was investigated using far- and near-UV CD spectroscopy, fluorescence spectroscopy, and DSC. As typical examples, far-UV CD spectra of PCPI 8.3 and PCPI 9.4 at various temperatures (pH 4.0) are shown in **Figure 6**. Similar results were also obtained for PCPI 8.6. No changes in intensity occurred up to 60 °C. With increasing temperature above 60 °C, the absolute intensities at 200 and 228 nm decreased and were inverted.

Figure 7A shows the ellipticity of PCPI 8.3, 8.6, and 9.4 at 222 nm as a function of temperature. It can be observed that the shapes of the thermal unfolding curves of PCPI 8.6 and 9.4 are similar and that the changes in secondary structure for both isoforms occur in a very narrow temperature range (approximately 4.5 °C). The ellipticity at 222 nm for PCPI 8.6 (pH 4.0) showed changes between 68.5 and 73.0 °C, with a midpoint at 70.3 °C, whereas for PCPI 9.4, the changes occurred between 66.8 and 71.6 °C, with a midpoint at 69.4 °C. For PCPI 8.3, the changes occur in a broader temperature range (around 9 °C) (**Figure 7A**). In the secondary structure of PCPI 8.3, the changes take place between 65.9 and 74.7 °C, with a midpoint at 70.0 °C. To monitor also the changes in tertiary structure, the tyrosine fluorescence emission at 300 nm was followed as a function of temperature. **Figure 7B** shows the thermal unfolding curves as followed by the tyrosine fluorescence emission intensity at 300 nm, as well as the unfolding curves

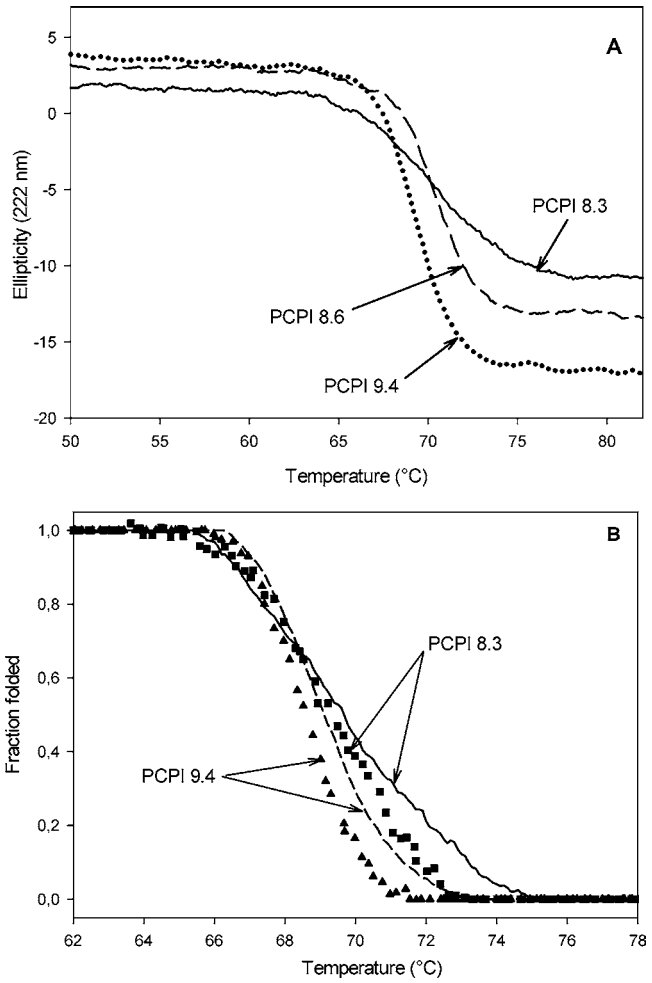

Figure 7. (**A**) Thermal unfolding curves of PCPI isoforms at pH 4.0, monitored by the far UV CD signal at 222 nm. (**B**) Thermal unfolding curves, monitored by the tyrosine fluorescence at 300 nm (■, PCPI 8.3; ▲, PCPI 9.4) and the far UV CD signal (222 nm).

followed by the CD signal at 222 nm, for PCPI 8.3 and 9.4. In the **Figure 7B**, the results are expressed as the fraction of PCPI in the folded state (*27*). The fluorescence unfolding curve for PCPI 8.6 was similar to that for PCPI 9.4 and is, therefore, not shown. It can be observed that the changes in the tertiary structure of PCPI 9.4 occur again in a very narrow temperature range (4 °C), whereas the changes for PCPI 8.3 occur in a broader temperature range (5.9 °C). The difference in the width of the temperature range of unfolding between the isoforms is, however, smaller than observed using far-UV CD. DSC measurements were performed in order to determine the energy content of the heat-induced conformational changes of PCPI isoforms (*23*). The DSC profiles of PCPI 8.6 and 9.4 at pH 4.0 each showed a symmetric peak with transition temperatures of 67.6 and 67.5 °C, respectively (**Figure 8**). The calorimetric enthalpies obtained for PCPI 8.6 and 9.4 are approximately 447 448 and 548 kJ/mol, respectively. The DSC profile of PCPI 8.3 showed a different shape (**Figure 8**). The peak is not symmetric due to a shoulder at 70 °C. These results indicate that either PCPI 8.3 consists of at least two parts that unfold more or less independently with temperature, or a stable intermediate is formed during the unfolding mechanism of PCPI 8.3. The calorimetric enthalpy for PCPI 8.3 is quite similar to that of PCPI 8.6 and 9.4 and amounts 497 kJ/mol. For all PCPI isoforms, rescanning the heated (70 °C for PCPI 8.6 and 9.4 and 74 °C for PCPI 8.3) samples resulted in less than 10% of

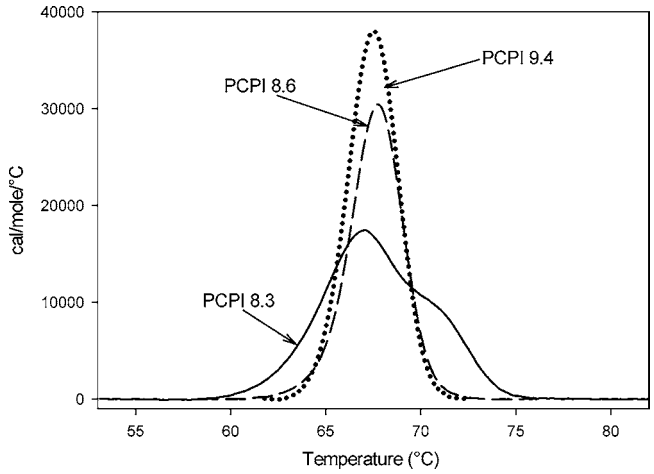

Figure 8. DSC thermograms of PCPI 8.3 (solid), PCPI 8.6 (dashes), and PCPI 9.4 (dot) at pH 4.0. Protein solutions were heated from 20 to 85 °C with a scan rate of 30 °C/h.

Table 1. Thermodynamic Parameters of PCPI Isoforms (Cv. Elkana) at pH 4.0

	transition temperature (°C)			ΔH_{cal}	ΔH_{vH}[a]	
	far UV CD	Tyr fluo	DSC	(kJ/mol)	(kJ/mol)	$\Delta H_{vH}/\Delta H_{cal}$
PCPI 8.3	70.0 ± 0.1	69.5 ± 0.2	67.0 ± 0.1	498 ± 11	449 ± 25	0.90 ± 0.10
PCPI 8.6	70.3 ± 0.2	69.6 ± 0.1	67.6 ± 0.1	448 ± 6	885 ± 44	1.97 ± 0.18
PCPI 9.4	69.4 ± 0.2	69.1 ± 0.2	67.5 ± 0.2	548 ± 8	909 ± 56	1.66 ± 0.18

[a] ΔH_{vH} was determined from the CD thermal unfolding curves.

the original peak area being recovered upon reheating, indicating that the transition is almost completely irreversible (data not shown) (*29*).

To obtain thermodynamic data from thermal unfolding CD curves of PCPI isoforms, the model given by van Mierlo et al. (*30*), based on thermodynamic equations (*31*, *20*), was used. Transition temperatures and calorimetric and Van't Hoff enthalpies as obtained from CD, fluorescence, and DSC measurements are shown in **Table 1**. The ratios of the Van't Hoff enthalpy and the calorimetric enthalpy are also shown in this table. This ratio differs from 1 for two of the three isoforms and ranges from 0.9 for PCPI 8.3 to approximately 2 for PCPI 8.6. These results indicate that PCPI does not unfold via a simple two-state mechanism but that at least one intermediate is present (*29*, *32*).

Concentration and Scan Rate Dependency. Figure 9A shows the transition temperature as well as the calorimetric enthalpy as a function of the protein concentration for the three PCPI isoforms, as obtained by DSC. It can be clearly seen that the transition temperature decreases when the protein concentration increases, whereas the ΔH_{cal} remains constant. These results indicate that increasing protein concentration leads to a more extensive aggregation even though the peak remains symmetric (*29*). The changes in transition temperature with protein concentration followed the same trend for all three isoforms.

To examine the aggregation behavior of PCPI 9.4, samples with concentrations between 0.2 and 1 mg/mL were studied by gel filtration, after heating at 85 °C (**Figure 9B**). The results show that heating leads to the formation of aggregates at all concentrations tested. Even at the lowest concentration (0.2 mg/mL), aggregation occurred and no nonaggregated PCPI was observed (Ve = 15 mL). However, also a peak, eluting at 17.5 mL, appeared, indicating a molecular mass of approximately 7 kDa. Similar results were obtained for PCPI 8.3 and 8.6,

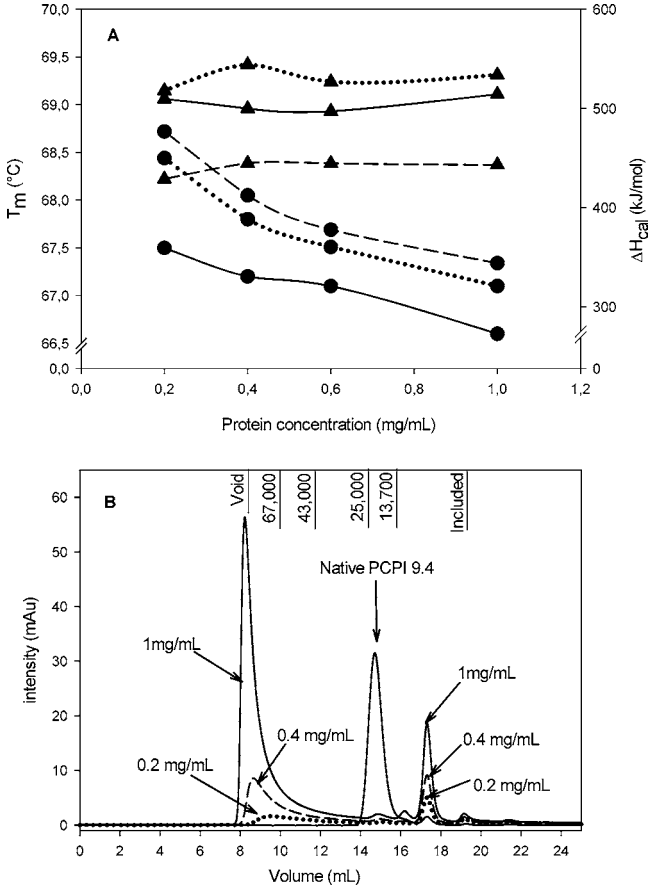

Figure 9. (**A**) Effect of protein concentration on the transition temperature (●) and the ΔH_{cal} (▲) for PCPI 8.3 (solid), PCPI 8.6 (dashes), and PCPI 9.4 (dot). Protein solutions were heated from 20 to 85 °C with a scan rate of 30 °C/h. (**B**) Gel filtration of PCPI after heating from 20 to 85 °C at different protein concentrations.

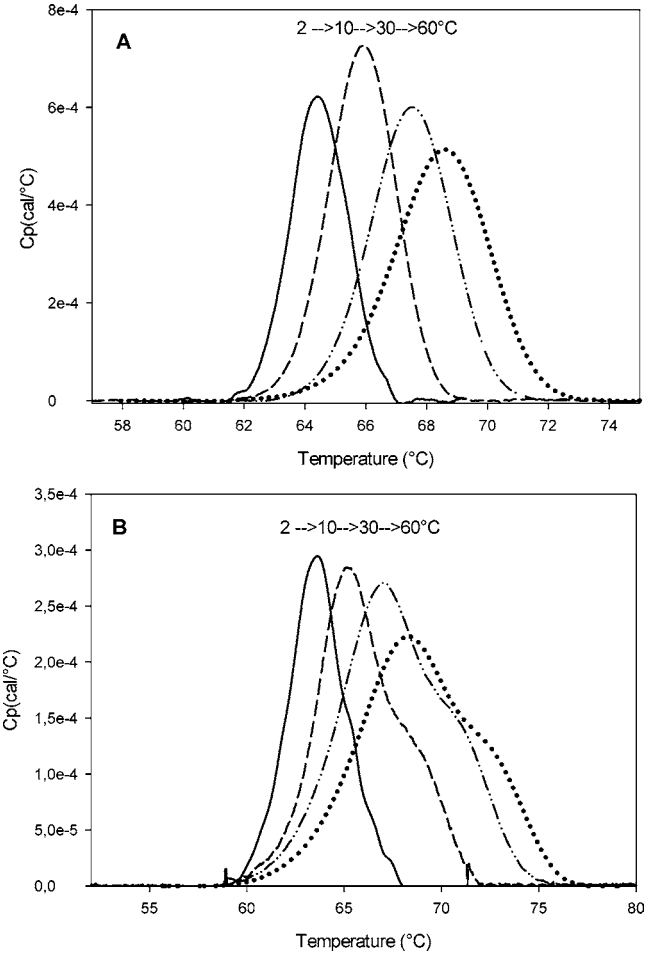

Figure 10. DSC thermograms of PCPI 9.4 (**A**) and PCPI 8.3 (**B**) at 2 (solid), 10 (dashes), 30 (dots and dashes), and 60 (dot) °C/h.

including the appearance of the 7 kDa peak (data not shown). The origin of the 7 kDa peak remains unclear, and further characterizations would be needed to determine the nature of this peak. One hypothesis is that a flexible part of the protein is cleaved during heating. Like all Kunitz type inhibitors, PCPI isoforms contain four cysteine residues forming two disulfide bridges. Experiments in the presence of DTT showed that aggregation is not occurring (data not shown). Therefore, aggregation seems to occur via a specific mechanism, which seems to involve disulfide interchanges. In comparison to PSPI (*17*), the end product is not a tetrameric form of the protein and may not be of one single population. Further analyses have to be performed in order to characterize the aggregates.

To establish equilibrium between the native and the unfolded state at all temperatures, the heating rate should be much lower than the folding/unfolding rates (*33*). Therefore, PCPI isoforms were heated at scan rates between 2 and 60 °C/h.

Figure 10 shows thermograms of PCPI 8.3 and 9.4 at various scan rates. For PCPI 9.4, the peak remained symmetric but became less sharp and shifted to a higher temperature, with an increasing scan rate in the range of 2−60 °C/h (**Figure 10A**). A similar, but even larger, effect of scan rate was observed for PCPI 8.3 (**Figure 10B**). The transition temperatures for all three isoforms decreased with decreasing scan rate, whereas the calorimetric enthalpies increased from 280 to 460, from 210 to 400, and from 385 to 530 kJ/mol for PCPI 8.3, 8.6, and 9.4, respectively. These results indicate that no equilibrium is reached, even at the lowest scan rate.

DISCUSSION

PCPI: Its Similarity to PSPI. Previously, PSPI was classified as a β-II protein (*17*). The far-UV CD spectra of all investigated PCPI isoforms show extremes at approximately 200 and 228 nm, similar to the spectra obtained for PSPI (*17*). Together with the sharp peaks in the near-UV CD spectra and the narrow temperature range in which thermal unfolding occurs, this indicates that also PCPI can be classified as a β-II protein. Moreover, the large similarity of both the far-UV CD and the infrared spectra of PCPI to those of PSPI and to those of another β-II protein, the Kunitz type inhibitor STI, confirm this classification.

The maximum in the far-UV CD spectrum at 228 nm has been observed for various protease inhibitors such as STI (*34*) and clitocypin, a cysteine protease inhibitor from mushroom (*35*). This positive maximum seems to be a common characteristic of many protease inhibitors belonging to the β-II protein class. Therefore, the common structure (fold), consisting of distorded (not plan) β-sheets, of the protease inhibitors from the β-II protein subclass may be responsible for this positive maximum.

Comparison between PCPI Isoforms. The results presented indicate that the thermal unfolding of PCPI occurs via a nontwo-state mechanism in which at least one intermediate is formed, thus preventing the use of equilibrium thermodynamics. Interpretation of the thermal unfolding data is further complicated by the occurrence of aggregation, which, especially at low scan

rates, increases the apparent cooperativity of the unfolding ($\Delta H_{vH}/\Delta H_{cal}$) and makes the system kinetically rather than thermodynamically controlled (*36*).

In this study, several differences between the three isoforms of PCPI were observed. PCPI 8.6 and 9.4 gave in all experiments very similar results, while in some cases PCPI 8.3 showed a different behavior. PCPI isoforms showed similar structural properties, although the zero crossing in the far-UV CD spectrum of PCPI 8.3 indicates that PCPI 8.3 may have a slightly different secondary structure. No differences between the three isoforms could be observed in the ATR-IR spectra.

The differences between these isoforms became more apparent upon thermal unfolding. The changes in secondary and tertiary structure occur in a broader temperature range for PCPI 8.3 than for the other two isoforms. The absence of complete overlap between the temperature ranges in which the secondary and tertiary structures of PCPI isoforms unfold indicates the presence of a stable intermediate of a "molten globule" type (*37*, *38*).

It is difficult to explain the differences in behavior upon thermal unfolding between the PCPI isoforms since they show a very high similarities at secondary and tertiary levels. The fact that the amino acid sequences of PCPI 8.6 and 9.4 are unknown makes it even more complicated. However, PCPI 8.3 shows slightly less sharp peaks in the near-UV CD spectra, which may indicate a less compact structure than the one of PCPI 8.6 and 9.4. This might be an explanation for the thermal unfolding occurring via a broader temperature range for PCPI 8.3. However, more precise characterizations of PCPI isoforms upon heating have to be performed.

NOTE ADDED AFTER ASAP PUBLICATION

In the original ASAP posting on June 11, 2005, reference *36* was left out. This was corrected on June 23, 2005.

LITERATURE CITED

(1) Ryan, C. A. Proteolytic enzymes and their inhibitors in plant. *Annu. Rev. Plant Physiol.* **1977**, *24*, 173−196.

(2) Garcia-Olmeda, F.; Sakedo, G.; Sanchez-Monge, R.; Gomez, L.; Royo, J.; Carbonero, P. Plant proteinaceous inhibitors of proteinases. *Oxf. Surv. Plant Cell Mol. Biol.* **1987**, *4*, 275−334.

(3) Lisinska, G.; Leszczynski, W. *Potato Science and Technology*; Elsevier Applied Science: London, 1989.

(4) Pouvreau, L.; Gruppen, H.; Piersma, S. R.; van den Broek, L. A. M.; van Koningsveld, G. A.; Voragen, A. G. J. Relative abundance and inhibitory distribution of protease inhibitors in potato juice from cv. Elkana. *J. Agric. Food Chem.* **2001**, *49*, 2864−2874.

(5) Turk, V.; Turk, B.; Guncar, G.; Turk, D.; Kos, J. Lysosomal cathepsins: Structure, role in antigen processing and presentation, and cancer. *Adv. Enzyme Regul.* **2002**, *42*, 285−303.

(6) Kos, J.; Stabuc, B.; Schweiger, A.; Krasovec, M.; Cimerman, N.; Kopitar-Jerala, N.; Vrhovec, I. Cathepsins B, H, and L and their inhbitors stefin A and cystatin C in sea of melanoma patients. *Clin. Cancer Res.* **1997**, *3*, 1815−1822.

(7) Gruden, K.; Strukelj, B.; Ravnikar, M.; Poljsak-Prijatelj, M.; Mavric, I.; Brzin, J.; Pungercar, J.; Kregar, I. Potato cysteine proteinase inhibitor gene family: Molecular cloning, characterisation and immunocytochemical localisation studies. *Plant Mol. Biol.* **1997**, *34*, 317−323.

(8) Knorr, D.; Kohler, G. O.; Betschart, A. A. Potato protein concentrates: the influence of various methods of recovery upon yield, compositional and functional characteristics. *J. Food Process. Preserv.* **1977**, *1*, 235−247.

(9) Krizaj, I.; Drobnic-Kosorok, M.; Brzin, J.; Jerala, R.; Turk, V. The primary stucture of inhibitor of cysteine proteinases from potato. *FEBS Lett.* **1993**, *333*, 15−20.

(10) Bradford, M. M. A rapid and sensitive method for the quantification of microgram quantities of protein utilizing the principle of protein-dye binding. *Anal. Biochem.* **1976**, *72*, 248−254.

(11) de Jongh, H. H. J.; Goormachtigh, E.; Killian, A. Analysis of circular dichroism spectra of oriented protein−lipid complexes: Toward a general application. *Biochemistry* **1994**, *33*, 14521−14528.

(12) Greenfield, N. J.; Fasman, G. D. Computed circular dichroism spectra for evaluation of protein conformation. *Biochemistry* **1969**, *8*, 4108−4116.

(13) Chang, C. T.; Wu, C.-S. C.; Yang, J. T. Circular dichroic analysis of protein conformation: Inclusion of the b-turns. *Anal. Biochem.* **1978**, *91*, 13−31.

(14) van Mierlo, C. P. M.; de Jongh, H. H. J.; Visser, A. J. W. G. Circular dichroism of proteins in solution and at interfaces. In *Physical Chemistry of Biological Interfaces*; Baszkin, A., Norde, W., Eds.; Marcel Dekker: New York, 2000.

(15) Teale, F. W. J. The ultraviolet fluorescence of proteins in neutral solution. *Biochem. J.* **1960**, *76*, 381−388.

(16) Ruan, K.; Li, J.; Liang, R.; Xu, C.; Yu, Y.; Lange, R.; Balny, C. A rare protein fluorescence behavior where the emission is dominated by tyrosine: Case of the 33-kDa protein from spinach photosystem II. *Biochem. Biophys. Res. Commun.* **2002**, *293*, 597−597.

(17) Pouvreau, L.; Gruppen, H.; van Koningsveld, G. A.; van den Broek, L. A. M.; Voragen, A. G. J. Conformational stability of the potato serine protease inhibitor group (cv. *Elkana*). *J. Agric. Food Chem.* **2004**, *52*, 7704−7710.

(18) Kelly, S. M.; Price, N. C. The application of circular dichroism to studies of protein folding and unfolding. *Biochim. Biophys. Acta* **1997**, *1338*, 161−185.

(19) Brzin, J.; Popovic, T.; Drobnic-Kosorok, M.; Kotnik, M.; Turk, V. Inhibitors of cysteine proteinases from potato. *Biol. Chem. Hoppe. Seyler* **1988**, *369*, 233−238.

(20) Pace, C., N.; Shirley, B. A.; Thomson, J. A. Measuring the conformational stability of a protein. In *Protein Structure; A Practical Approach*; Creighton, T. E., Eds.; IRL Press: Oxford, 1989.

(21) Vladimorov, M. V.; Burstein, E. A. Luminescent spectra of aromatic amino acids and proteins. *Biophysika* **1960**, *5*, 385−392.

(22) Haris, P. V.; Severcanb, F. FTIR spectroscopic characterization of protein structure in aqueous and nonaqueous media. *J. Mol. Catal.* **1999**, *7*, 207−221.

(23) De Meester, P.; Brick, P.; Lloyd, L. F.; Blow, D. M.; Onesti, S. Structure of the Kunitz-type soybean trypsin inhibitor (STI): Implication for the interactions between members of the STI family and tissue-plasminogen activator. *Acta Crystallogr., Sect. D: Biol. Crystallogr.* **1998**, *54*, 589−597.

(24) Song, H. K.; Suh, S. W. Kunitz-type soybean trypsin inhibitor revisited: refined structure of its complex with porcine trypsin reveals an insight into the interaction between a homologous inhibitor from *Erythrina caffra* and tissue-type plasminogen activator. *J. Mol. Biol.* **1998**, *275*, 347−363.

(25) Goormaghtigh, E.; Cabiaux, V.; Ruysschaert, J.-M. Determination of soluble and membrane protein structure by Fourier transform infrared spectroscopy. III. Secondary structures. *Subcell. Biochem.* **1994**, *23*, 405−450.

(26) Tetenbaum, J.; Miller, L. M. A new spectroscopic approach to examining the role of disulfide bonds in the structure and unfolding of soybean trypsin inhibitor. *Biochemistry* **2001**, *40*, 12215−12219.

(27) van Mierlo, C. P. M.; Steensma, E. Protein folding and stability investigated by fluorescence, circular dichroism (CD), and nuclear magnetic resonance (NMR) spectroscopy: The flavodoxin story. *J. Biotechnol.* **2000**, *79*, 281−298.

(28) Boye, J. I.; Ma, C.-Y.; Harwalkar, V. R. Thermal denaturation and coagulation of proteins. In *Food Proteins and Their Applications*; Damodaran, S., Parat, A., Eds.; Marcel Dekker Inc.: New York, 1997.

(29) Makhatadze, G. I. Measuring protein thermostability by differential scanning calorimetry. In *Current Protocols in Protein Science*; Coligan, J. E., Dunn, B. M., Ploegh, H. L., Speicher, D. W., Wingfield, P. T., Eds.; John Wiley and Sons: New York, 1998; pp 7.9.1−7.9.14.

(30) van Mierlo, C. P. M.; van Dongen, W. M. A. M.; Vergeldt, F.; van Berkel, W. J. H.; Steensma, E. The equilibrium unfolding of *Azotobacter vinelandii* apoflavodoxin II occurs via a relatively stable folding intermediate. *Protein Sci*. **1998**, *72*, 331−2344.

(31) Becktel, W. J.; Schellman, J. A. Protein stability curves. *Biopolymers* **1987**, *26*, 1859−1877.

(32) Burova, T. V.; Grinberg, N. V.; Grinberg, V. Y.; Tolstoguzov, V. B. Binding of odorants to individual proteins and their mixtures. Effects of protein denaturation and association A plasticized globule state. *Colloid Polym. Sci.* **2003**, *213*, 235−244.

(33) Yu, Y.; Makhatadze, C.; Pace, N.; Privalov, P. L. Energetics of ribonclease T1 structure. *Biochemistry* **1994**, *33*, 3312−3319.

(34) Wu, J.; Yang, J. T.; Wu, C.-S. C. β-II conformation of all-β proteins can be distinguished from unordered form by circular dichroism. *Anal. Biochem.* **1992**, *200*, 359−364.

(35) Kidric, M.; Fabian, H.; Brzin, J.; Popovic, T.; Pain, R. H. Folding, stability, and secondary structure of a new cysteine dimeric proteinase inhibitor. *Biochem. Biophys. Res. Commun.* **2002**, *297*, 962−967.

(36) Hoffmann, M. A. M.; van Miltenburg, J. C.; van Mil, P. J. J. M. The suitability of scanning calorimetry to investigate slow irreversible protein denaturation. *Thermochim. Acta*, **1997**, *306*, 45−49.

(37) Ohgushi, M.; Wada, A. 'Molten-globule state': A compact for m of globular proteins with mobile side chains. *FEBS Lett.* **1983**, *164*, 21−24.

(38) Dolgikh, D. A.; Kolomiets, A. P.; Bolotina, I. A.; Ptitsyn, O. B. 'Molten-globule' state accumulates in carbonic anhydrase folding. *FEBS Lett.* **1984**, *165*, 88−92.

Received for review February 10, 2005. Revised manuscript received May 9, 2005. Accepted May 17, 2005.

JF050306V